ACS APPLIED MATERIALS & INTERFACES

Research Article

www.acsami.org

Creation of Hydrophilic Nitric Oxide Releasing Polymers via Plasma Surface Modification

A. Pegalajar-Jurado,[†] J. M. Joslin,[†] M. J. Hawker,[†] M. M. Reynolds,[†,‡] and E. R. Fisher*[,†]

[†]Department of Chemistry and [‡]School of Biomedical Engineering, Colorado State University, Fort Collins, Colorado 80523, United States

Supporting Information

ABSTRACT: Herein, we describe the surface modification of an *S*-nitrosated polymer derivative via H_2O plasma treatment, resulting in polymer coatings that maintained their nitric oxide (NO) releasing capabilities, but exhibited dramatic changes in surface wettability. The poly(lactic-*co*-glycolic acid)-based hydrophobic polymer was nitrosated to achieve a material capable of releasing the therapeutic agent NO. The NO-loaded films were subjected to low-temperature H_2O plasma treatments, where the treatment power (20−50 W) and time (1−5 min) were varied. The plasma treated polymer films were superhydrophilic (water droplet spread completely in <100 ms), yet retained 90% of their initial *S*-nitrosothiol content. Under thermal conditions, NO release profiles were identical to controls. Under buffer soak conditions, the NO release profile was slightly lowered for the plasma-treated materials; however, they still result in physiologically relevant NO fluxes. XPS, SEM-EDS, and ATR-IR characterization suggests the plasma treatment resulted in polymer rearrangement and implantation of hydroxyl and carbonyl functional groups. Plasma treated samples maintained both hydrophilic surface properties and NO release profiles after storage at −18 °C for at least 10 days, demonstrating the surface modification and NO release capabilities are stable over time. The ability to tune polymer surface properties while maintaining bulk properties and NO release properties, and the stability of those properties under refrigerated conditions, represents a unique approach toward creating enhanced therapeutic biopolymers.

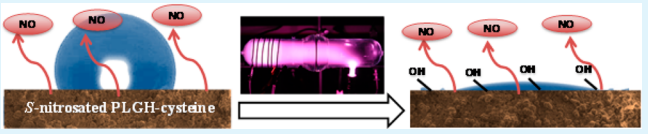

KEYWORDS: *nitric-oxide-releasing materials, plasma treatments, PLGH, cysteine, nitrosation*

1. INTRODUCTION

Current medical device surfaces are plagued by biofouling issues, predominantly blood clot formation[1−3] and bacterial infection.[4,5] Functional materials are critical to modulate biological responses at the material-biology interface to combat the processes that lead to severe medical complications that are largely driven by the physicochemical properties of a material's surface.[6,7] Additionally, surface properties control cell attachment and proliferation, critical factors for improving the biocompatibility of a plethora of medical devices.[8] Properties that control the microorganism−surface interactions include surface chemical composition, surface free energy, surface topography, and surface wettability.[9] It is likewise important to acknowledge that the microorganism surface hydrophobicity, charge, and electronegativity also play an important role on microorganism−material surface interactions.[10,11] Nonetheless, manipulation of surface chemistry and wettability of synthetic materials is the most accessible path for controlling microorganism−surface interactions and enhancing biocompatibility. Therefore, the ability to tune material surface properties while retaining the desirable bulk properties can allow for limited bacterial attachment to prevent infection, with simultaneous favoring of cell attachment and proliferation to promote material integration and healing processes. Moreover, the incorporation of therapeutic agents in the bulk material for controlled release, such as antithrombogenic, reendothelialization, and antibiotic drugs, can help to prevent clot formation, promote wound-healing, and fight potential infections, respectively.[12−15]

Surface modification represents a passive approach to control microorganism attachment and adhesion processes, whereas therapeutic release approaches aim to actively eradicate bacteria and enhance cellular proliferation. Thus, a material that combines these tactics would represent an advanced functional material that targets different biological mechanisms, thereby offering precise control over physiological responses at the biomaterial surface. Notably, such ability to control multiple pathways associated with biocompatibility is key for developing enhanced materials for applications such as tissue engineering, wound dressing fabrication, and antimicrobial materials development.

Surface chemical composition and wettability greatly influence the deposition of biological components. For example, Arima and Iwata highlighted the effect of terminal functional groups for self-assembled monolayers (SAMs) on protein adsorption and cell adhesion.[8] Increased protein adsorption was observed for surfaces with increasing hydrophilicity for many functional groups (e.g., OH, CH_3/COOH). Additionally, endothelial and epithelial cells attached and spread significantly on surfaces with increased hydrophilicity

Received: April 1, 2014
Accepted: July 15, 2014
Published: July 15, 2014

(i.e., increase in surface COOH or NH_2), which promotes wound healing and device integration. Parreira et al. reported a correlation between the presence of different functional groups on a surface (i.e., CH_3 and OH) and wettability with the increase or reduction of *Helicobacter pylori* attachment.[16] Although the 17875/Leb strain showed a distinctive preference for hydrophilic surfaces, the remainder of the *H. pylori* strains exhibited opposite behavior, indicating bacteria attachment to surfaces is both surface and strain dependent. These observations emphasize the need for materials with tunable surface chemical composition and wettability depending upon the intended application of the material as protein, cell, and bacteria behavior changes depending on surface properties.

Several techniques are used to modify surface properties of different materials, including polymer grafting, biomolecule immobilization, and plasma treatment.[17,18] Plasma treatments can be a reproducible approach for modifying surface chemical composition and wettability without changing the bulk material properties, using a sterile, solvent-free, and low-temperature environment.[19] Plasmas also afford the ability to tune surface chemical composition and wettability by deposition of thin films or via implantation of desirable oxygen and nitrogen-containing functional groups.[20] In both approaches, several process variables can be adjusted (e.g., precursor, applied power, treatment time, pressure, substrate position, and gas flow rate) to impact the efficacy of the plasma treatment. Previously, we and others have used H_2O plasmas to increase surface wettability of different materials by implanting OH groups.[21−24] With hydrophobic polysulfone membranes, not only did H_2O plasma treatment permanently improve wettability, but the change affected the entire membrane cross section, lasting for >2 years. Lee et al. highlighted an increase in cell adhesion, spreading, and growth for H_2O plasma treated polymers.[21] Thus, H_2O plasma treatment is a highly suitable methodology for changing wettability toward enhancing cell−surface compatibility. However, unfavorable effects can be promoted by improved wettability, including biofilm formation and thrombosis. Tuning surface wettability alone is, therefore, insufficient for developing targeted biocompatible materials and may need to be combined with additional approaches, including release of a therapeutic agent.

One therapeutic agent that has demonstrated excellent antithrombogenic and antimicrobial properties is nitric oxide (NO).[25] As a result of its release from endothelial cells to regulate platelet and clotting activity,[26,27] as well as its natural role in fighting infection[28] and promoting wound-healing,[29−31] NO is a multifunctional therapeutic agent. Many material platforms have been developed with NO-release capability and improved biocompatibility in comparison to control materials.[6,32−35] The use of NO as the agent of choice for drug-eluting polymer systems is distinctive because NO can target multiple physiological actions, compared to other agents, such as heparin or antibiotics, which target only a single function. Current objectives in the field include temporal and spatial control over NO release, namely, achieving appropriate NO fluxes for the intended application and ensuring that NO release occurs directly at the material−biology interface for a localized effect. Although some NO-releasing materials such as hydrogels are hydrophilic,[36] unfortunately, many that have high antimicrobial activity are hydrophobic,[6,32,34,37,38] thereby potentially limiting the number of applications in which these materials would be useful.[39]

An ideal NO releasing material would exhibit (a) bulk mechanical and chemical properties to ensure stability over the device lifetime when exposed to bodily fluids; (b) controllable NO release directed at the microorganism−material interface; and (c) controlled surface hydrophilicity. Although plasma treatments have been used to modify the surface properties of drug-releasing polymers,[40−42] to date, no attempts to modify the surface properties of an NO releasing polymer while maintaining the bulk properties of the material have been reported. Therefore, the combined ability to tune both the NO delivery as well as the surface properties represents a unique approach to potentially creating NO releasing biopolymers that can modulate biological interactions while fighting infection and thrombus formation.

We recently reported on a multiblock polymer system based upon the United States Food and Drug Administration (FDA) approved poly(lactic-*co*-glycolic acid) (PLGH) polymer.[43] The polymer backbone was synthesized with covalent attachments of thiol groups, which were subsequently nitrosated to results in *S*-nitrosated PLGH derivatives with the capability to release NO. The NO reservoir and ultimately the NO release kinetics were controlled based upon the functionality associated with the thiol site. Moreover, we developed robust methods to enable the characterization and quantification of the *S*-nitrosothiol (RSNO) moieties on the polymer, which are the source of NO. The surface properties of these NO-releasing materials were not, however, ideal for enhancing cell compatibility. Although nondrug releasing PLGA systems have been plasma treated to improve the polymer surface properties for specific biological applications,[44−46] the surface modification of a material that releases NO has not previously been reported.

Here, we expand the utility of the *S*-nitrosated PLGH system by changing the surface properties of the material by plasma treatment. Using inductively coupled H_2O plasmas, we assessed the effects of two process parameters, applied rf power (20−50 W) and treatment time (1−5 min), on the surface properties of *S*-nitrosated PLGH polymer thin films. As a result of plasma treatment, the surface chemical composition and functional group distribution changed minimally, but surface wettability underwent a dramatic shift from hydrophobic to completely wetting while retaining NO release properties. Overall, this work highlights that we have developed a methodology that allows tuning the surface properties of NO releasing materials while maintaining the desirable therapeutic activity, thereby offering a significant advancement toward developing functional biomaterials, including coatings for wound dressing, bandages, and stitches.

2. EXPERIMENTAL SECTION

2.1. Materials. All reagents to prepare the PLGH-cysteine polymer are described elsewhere.[47] The *t*-butyl nitrite (90%) was obtained from Aldrich (St. Louis, MO), the dichloromethane (DCM), methanol (MeOH), and potassium carbonate were obtained (ACS grade) from Fisher Scientific (Fair Lawn, NJ). The DCM and MeOH solvents were stored over 4 Å molecular sieves to keep dry. Anhydrous ethanol was obtained from Pharmco Products, Inc. (Brookfield, CT) and AAPER alcohol from Pharmco-AAPER (Shelbyville, KY).

2.2. Preparation of *S*-Nitrosated PLGH-Cysteine Films. The PLGH-cysteine derivative (structure shown in Figure 1) was prepared according to a previously reported synthetic scheme, and the structure of the polymeric materials used in this study was determined to be comparable to the previously reported materials via NMR.[43,48] Briefly, a carboxyl-functionalized polymer was prepared from L-lactide,

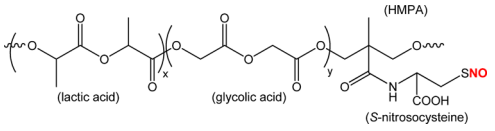

Figure 1. Structure of *S*-nitrosated poly(lactic-*co*-glycolic acid)-cysteine (PLGH-cysteine).

glycolide, and 2,2-bis(hydroxymethyl propionic acid) (HMPA) via a ring-opening melt polymerization using a stannous octoate catalyst. The carboxyl group of the HMPA polymer segment was further functionalized with cysteine after *N*-hydrosuccinimide activation. The cysteine group was covalently attached to the PLGH backbone through an amide linkage.

A modified Ellman's assay was performed to quantify the extent of polymer thiolation. PLGH-cysteine samples were prepared at 0.5 mg mL^{-1} in 2 MeOH/1 DCM. Cysteamine standards were prepared at 0–250 μM in solvent containing 0.5 mg mL^{-1} PLGH. Each standard and sample (1 mL) was treated with 5,5′-dithiobis(2-nitrobenzoic acid), the Ellman's reagent, (10 mM, 1 mL) in the presence of 200 μL of potassium carbonate-saturated solution. The absorbance of each solution was recorded at 414 nm on a Thermo Evolution 300 UV–vis spectrophotometer, and the concentration of thiol associated with the polymer was determined from the corresponding cysteamine calibration curve (see Supporting Information, Figure S1).

Nitrosation of the PLGH-cysteine to form the *S*-nitrosated polymer derivative was accomplished by using *t*-butyl nitrite as the nitrosating agent. The PLGH-cysteine (50 mg) was dissolved in 2 MeOH/1 DCM (2 mL) in an amber EPA-certified vial (Fisher Scientific, NJ). To facilitate nitrosation, the *t*-butyl nitrite (8.4 mg in 1 mL of 2 MeOH: 1 DCM) was added to the polymer solution. The polymer solution was stirred and protected from light for 4 h, followed by a 2 h vacuum step to remove the solvent and residual *t*-butyl nitrite. The final product was a pink-colored powder which is a visual confirmation of the success of the nitrosation process.

Films of the *S*-nitrosated PLGH-cysteine were prepared by redissolving the polymer in 2 MeOH/1 DCM (50 mg mL^{-1}). Aliquots of the polymer solution (100 μL) were dispensed on round glass slides (VWR micro cover glass, 12 mm diameter, 113 mm^2 area) and dried overnight protected from light. The mass of each individual film was determined by subtracting the mass of the glass slide from the mass of the slide containing the polymer film. All *S*-nitrosothiol and NO values were normalized by the mass of the film (see below). To consider film thickness, an important parameter associated with NO releasing materials,[3] digital calipers (Fisher Scientific) were used to measure the thickness of the slide before and after film deposition. An average film thickness of 0.057 ± 0.008 mm was determined.

2.3. Plasma Treatment of *S*-Nitrosated PLGH-Cysteine Films. H_2O plasma treatments on *S*-nitrosated PLGH-cysteine films were performed using a home-built glass tubular reactor, which was inductively coupled via a Ni-plated copper coil. Radio frequency (rf, 13.56 MHz) plasma power was applied through a matching network, and varied between plasma treatments (applied rf power (P) = 20, 30, or 50 W). Reactor pressure was monitored using a Baratron capacitance manometer, and was allowed to stabilize at 200 mTorr above base reactor pressure before plasma ignition. A deionized water sample (Millipore, 18 mΩ cm) was subjected to three freeze–pump–thaw cycles to remove trapped atmospheric gases prior to use and was introduced into the reactor from a 50 mL Pyrex side arm vacuum flask with a Teflon stopcock. Substrates were placed on a clean glass slide 16 cm downstream from the coil for each treatment, with treatment times of 1, 3, or 5 min. Typically, nine substrates were treated simultaneously for analysis. The plasma treated films were subsequently analyzed for *S*-nitrosothiol content and NO releasing capabilities. Surface and bulk analyses (water contact angle, X-ray photoelectron spectroscopy, scanning electron microscopy-energy dispersive X-ray spectroscopy, Fourier transform infrared spectroscopy, and optical profilometry) were also performed to assess the wettability, composition, and morphology of the polymer films prior to and after treatment.

2.4. *S*-Nitrosothiol Characterization. To quantify the *S*-nitrosothiol content for the polymer films before and after plasma treatments, solution phase UV–vis measurements were performed. The polymer-coated glass slide was added to an amber EPA-certified vial and the polymer dissolved in 2 MeOH/1 DCM (1 mL). The polymer solution was added to a quartz cuvette (1 cm path length) for subsequent UV–vis analysis on an Evolution 300 spectrophotometer (Thermo Electron). To consider the contribution of the blank polymer absorbance, non-nitrosated PLGH-cysteine controls were prepared (2, 3.5, 5 mg mL^{-1}). From this calibration curve, the blank response is subtracted from the nitrosated polymer scan based upon the polymer concentration (see Supporting Information, Figure S2).

2.5. NO Release Analysis. The NO releasing capabilities of the polymer films before and after plasma treatments were assessed using nitric oxide analyzers (NOAs, Sievers 280i, GE, Boulder, CO). The NOAs are highly selective and sensitive for the direct chemiluminescent detection of NO.[49] As a simplified approach to monitor any changes on the NO release profile after plasma treatment, the polymer coated glass substrate was placed in an NOA cell and NO measurements were collected in 5 s intervals over the course of 12 h under dry conditions while the NOA cell was placed in a 37 °C water bath. Although the duration of the NO release can exceed 12 h, any changes attributed to the plasma treatment will be highlighted during this initial release period. Additional studies were performed to analyze the NO release for films exposed to a phosphate buffered saline (PBS) soak for a prolonged time period. The PBS was prepared from tablet (OmniPur, EMD Millipore) to yield a pH 7.4 solution. To perform these experiments, a film was placed in the bottom of an NOA cell, and 4.5 mL of PBS was added at the start of the run. Each film underwent NO analysis for a 24 h time period under PBS soak.

2.6. Water Contact Angle Analysis. Static water contact angle (WCA) measurements were collected using a Krüss DSA 30S contact angle goniometer to assess wetting properties. A 6 μL drop of deionized water (Millipore, 18 mΩ cm) was placed on the substrate. High-speed video recording was performed on each sample (64 frames per second for 10 s). For untreated samples, static WCA values are reported. Due to the high hydrophilicity of H_2O plasma treated samples, WCAs are reported in terms of water spreading time (ms). Effectively, treated samples have an equilibrium contact angle of 0°. All contact angle measurements were performed in triplicate to gauge reproducibility.

2.7. Surface Composition Analysis: XPS and SEM-EDS. X-ray photoelectron spectroscopy (XPS) analyses were performed on a PHI 5800 XPS system and provided information on surface composition and binding environments. Both an argon ion and an electron neutralizer were used to minimize sample charging. Survey spectra were collected from 10 to 1100 eV for 5 min, and high-resolution C 1s, O 1s, N 1s, and S 1s spectra were collected over a 15 min period.

A JEOL JSM-6500F scanning electron microscope (SEM) equipped with an energy dispersive spectrometer (EDS) was used to investigate the morphology and elemental mapping of both treated and untreated substrates. An accelerating voltage of 5.0 kV and a working distance of 10.0 mm were used for the analyses of untreated and treated substrates. Samples were grounded using conductive carbon tape. Three to five images were taken at 50× magnification, and EDS spectra were collected for 5 min.

2.8. Surface Morphology Analysis: SEM and Optical Profilometry. Surface morphology of the polymer films was assessed both visually and quantitatively by performing SEM and optical profilometry analysis. For SEM analysis, samples were grounded to a sample stage using conductive carbon tape. A JEOL JSM-6500F SEM was used to collect surface images at 100, 250, and 500× magnification. Three to five images were taken of each sample with an accelerating voltage of 1 kV and a working distance of approximately 10.0 mm.

To assess the surface roughness of the films before and after plasma treatment, a Zemetrics ZeScope optical profilometer was used. A single scan was collected for a 250 × 350 μm area using a 20×

magnification objective with a scan length of 150 μm in the z-axis and a signal threshold of 1.0%. Two scans were collected on each of three samples, for a total of $n = 6$ for each treatment. Both R_a and R_q values were determined from an average of the six scans using the ZeMaps measurement and analysis software, where R_a represents the arithmetic mean roughness across a sample scan and R_q represents the root-mean-square.

2.9. Bulk Composition Analysis: IR. To assess functional group incorporation (primarily OH) on the surface of the plasma treated film, IR analysis was performed on the untreated and treated PLGH-cysteine films. IR measurements were performed on a Nicolet 6700 FT-IR instrument equipped with an ATR sample stage with a ZnSe window. Scans were performed as an average of 64 scans with resolution of 1 (data spacing of 0.121 cm^{-1}). The ATR sample stage was cleaned with absolute, anhydrous ethanol (Pharmco Products, Inc.) between samples. Sample scans were performed in triplicate ($n = 3$) for each polymer sample. For these experiments, films were plasma treated and removed from the glass substrate to yield a polymer powder, wherein the surface was blended into the bulk of the polymer during removal.

3. RESULTS AND DISCUSSION

Previous studies have shown H_2O plasma treatments increase the hydrophilicity of polymer surfaces via functional group implantation (e.g., OH group implantation) and/or polymer reorganization.[22−24,50] Furthermore, depending upon the polymer, these changes can be relatively permanent, lasting from weeks to years.[23] This work explores the use of well-established H_2O plasma treatments to increase the hydrophilicity of an NO-releasing polymer, with the overarching goal of tuning surface properties without measurable morphological damage, while maintaining the bulk properties (e.g., NO-release profile) and ultimately achieving a biostable material with enhanced cell−surface affinity. Thus, the following sections detail our results for examining the various components of achieving this goal, including effects of plasma treatment on the surface and bulk composition, the surface contact angle and morphology, stability, and NO-releasing properties of the material.

3.1. Effect of Plasma Treatment on Composition of *S*-Nitrosated PLGH-Cysteine Films. To determine the effects of plasma treatments on polymer composition, both SEM-EDS and XPS analyses were performed. The C, O, and S elemental percentages derived from SEM-EDS analysis for each film are summarized in Table 1. Additional SEM-EDS data (spectra, images, and elemental ratios), are provided in the Supporting Information (see Figures S3−S5 and Table S1). Notably, these data suggest the oxygen and sulfur content of the materials does not change appreciably with plasma parameters. As SEM-EDS is not a surface sensitive technique (sampling depth of ~2 μm[51]), we are sampling more of the bulk material than the surface, and thus, these elemental composition ratios are essentially identical. This confirms that the bulk of the material is not experiencing significant alteration as a result of plasma treatment, a primary goal of these experiments.

Table 1. SEM-EDS Elemental Composition of Untreated and Plasma Treated *S*-Nitrosated PLGH-Cysteine Films[a]

plasma treatment				
applied rf power (W)	treatment time (min)	%C	%O	%S
untreated		60.5 ± 0.6	39.1 ± 0.4	0.4 ± 0.1
20	1	62.7 ± 0.4	37.2 ± 0.3	0.1 ± 0.1
20	3	61.7 ± 0.5	37.9 ± 0.4	0.4 ± 0.1
20	5	64.8 ± 0.7	35.1 ± 0.5	0.2 ± 0.1
30	5	60.3 ± 0.5	39.5 ± 0.4	0.2 ± 0.1
50	5	60.5 ± 0.7	39.1 ± 0.5	0.4 ± 0.1

[a]All analyses were performed for $N = 3$; the means ± standard deviation are reported.

XPS provides information about the surface chemical composition, as its sampling depth is only 5−10 nm.[52] XPS atomic composition ratios derived from C_{1s}, O_{1s}, and N_{1s} high resolution spectra of treated and untreated *S*-nitrosated PLGH-cysteine films are summarized in Table 2. High resolution S_{2p} spectra were also collected, though no appreciable change in S content was observed. Figure 2a highlights that the C/N ratio decreases with increasing treatment time at $P = 20$ W, indicating an increase in the surface nitrogen. No leaks were detected in the system during treatment; thus, it is unlikely that the additional nitrogen arose during the plasma treatment. There are, however, two other possible sources of this surface nitrogen: (1) the plasma treatment creates long-lived reactive radical sites at the surface of the polymer, which then react with atmospheric nitrogen upon exposure to air, or (2) the polymer reorganizes as a result of plasma treatment. Although the former has been observed previously,[53−55] the small changes observed in surface composition ratios upon sample aging (see section 3.6) suggest the latter explanation may be contributing to the observed nitrogen incorporation, as discussed below. The shallow reorganization of polymer chains when exposed to H_2O plasma treatments has been previously reported in the literature.[56] Here, the *S*-nitrosated PLGH-cysteine comprises a large hydrophobic backbone with hydrophilic pendant groups due to the cysteine residue. Consequently, we hypothesize that, in the H_2O vapor plasma environment, the *S*-nitrosocysteine pendant groups on the polymer are reorienting toward the water vapor environment, thereby exposing more of these hydrophilic microdomains at the surface.

For a fixed 5 min treatment time, an increase from $P = 20$ W to $P = 30$ W does not result in a statistically significant difference in the C/N ratio, whereas an additional increase in P to 50 W results in a small increase over the lower power treatments, Table 2. Compared to the untreated films (C/N = 30.6 ± 3.8), however, the C/N ratio for the 50 W treatment (21.5 ± 1.5) is not as low as those measured for the 20 W (17.1 ± 2.0) and 30 W (17.6 ± 1.8) treatments, which could indicate film etching is occurring in the higher P plasma.[50]

Although our XPS data support the possibility that reorientation of hydrophilic microdomains to the film surface may be occurring, implantation of hydrophilic functional groups that would improve the surface wettability is also an important surface modification to consider. Several reports demonstrate the use of H_2O plasma treatments to implant moieties with a variety of chemical environments (i.e., C═O, C−O, O−C═O) onto polymer surfaces.[22,24,50] For example, implantation of O-containing moieties into the *S*-nitrosated PLGH-cysteine film surface, can be tracked via XPS C/O ratio as a function of plasma treatment conditions, Figure 2b. These data show a general trend of decreasing C/O with increasing treatment time for $P = 20$ W, suggesting a relative increase in surface oxygen species with increasing plasma exposure. Although the C/O ratio declines slightly from untreated materials to films treated in $P = 30$ and 50 W systems, Table 2, this decrease is not very pronounced, possibly as a result of competitive etching under harsher plasma conditions. To further consider O implantation, the O/N and C/N ratios can

Table 2. XPS Atomic Composition Ratios of Untreated and Plasma Treated *S*-Nitrosated PLGH-Cysteine Films[a]

plasma treatment				
applied power (W)	treatment time (min)	C/O	O/N	C/N
untreated		1.67 ± 0.08	18.4 ± 2.5	30.6 ± 3.8
20	1	1.60 ± 0.05	16.4 ± 1.8	26.3 ± 2.7
20	3	1.48 ± 0.05	14.7 ± 1.5	21.7 ± 2.0
20	5	1.43 ± 0.05	12.0 ± 1.1	17.1 ± 2.0
30	5	1.51 ± 0.03	11.6 ± 1.3	17.6 ± 1.8
50	5	1.58 ± 0.03	13.6 ± 1.1	21.5 ± 1.5
20	5 (10 days aged)	1.54 ± 0.02	17.8 ± 1.4	27.5 ± 2.3

[a]All analyses were performed for $n = 6$; the means ± standard deviation are reported.

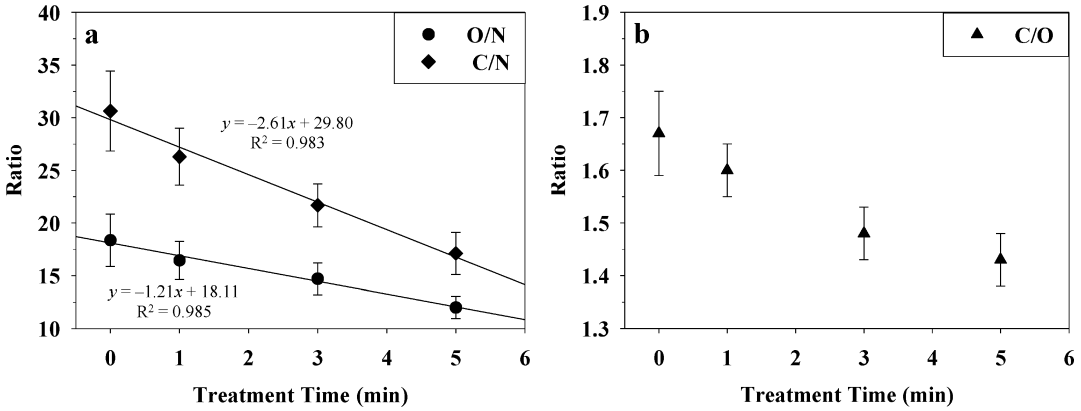

Figure 2. (a) O/N, C/N and (b) C/O as a function of plasma treatment time ($P = 20$ W) on *S*-nitrosated PLGH-cysteine substrates. Values are calculated from XPS elemental composition data (error bars represent ±1 standard deviation, $N = 6$). Additionally, linear regression fits with corresponding equations are shown for O/N and C/N in (a).

be compared as a function of treatment time. In Figure 2a, the slope of the regression line for C/N is steeper than that for O/N. This further suggests O incorporation is occurring, along with polymer rearrangement, to enhance the N signal at the surface of the films.

Despite the elemental ratios suggesting oxygen incorporation, these data do not provide information regarding changes in the oxygen binding environments after plasma treatment. To understand changes in surface chemical functionality as a function of plasma treatment time, high resolution C_{1s} XPS spectra were deconstructed for untreated and plasma treated samples (1 and 5 min treatment times, $P = 20$ W). This process involved fitting each C_{1s} spectrum with four unique binding environments, Figure 3a–c, corresponding to C–C/C–H, C═O, and O–C–C═O of the polymer backbone, and HN–C═O corresponding to the amide linkage of the *S*-nitrosocysteine residue. For the untreated polymer sample, the C═O binding environment comprises multiple functionalities, namely, the carboxylic acid moiety on the cysteine residues, as well as the multiple ester linkages in the lactic acid and glycolic acid portions of the polymer backbone, which results in a broadened peak relative to all other binding environments. The C_{1s} binding environments corresponding to the polymer backbone exhibit comparable intensities relative to each other, whereas the HN–C═O of the cysteine residue yields a smaller intensity. These proportions are consistent with the polymer structure (Figure 1).

The ratios between the C–C/C–H binding environment (285.0 eV) and the other C_{1s} binding environments were calculated, revealing a significant decrease in the C–C/C–H to HN–C═O ratio with increasing treatment time (Table 3). More specifically, the C–C/C–H to HN–C═O ratio is 10.12 ± 2.03 for the untreated sample, which decreases to 7.10 ± 0.71 for a 1 min treatment and to 4.55 ± 0.83 for a 5 min treatment. This increase in the relative intensity of the HN–C═O binding environment further supports the hypothesis that some rearrangement of the hydrophilic cysteine residues is occurring during plasma treatment. The other significant change in binding environments as a function of treatment time is the ratio of the sum of C═O-containing binding environments (C═O + HN–C═O) relative to the C–C/C–H binding environment (Figure 3d). Although these ratios for the untreated and 1 min plasma treated PLGH-cysteine films are within experimental error, that for the 5 min treated film is significantly lower. This implies that contributions from C═O environments increase with treatment time, suggesting extended plasma treatment promotes incorporation of carbonyl-containing functionalities such as aldehydes, ketone, and/or carboxylic acid groups.

Previous studies of H_2O plasma treatment of polysulfone and poly(ether imide) demonstrated implantation of O-containing groups at high P (20–200 W) arises from increased concentrations of OH and H radicals in the plasma.[50] Using optical emission spectroscopy (OES), a direct correlation was established between the intensity emission lines attributable to OH· and the concentration of oxygen in the material surface, as measured by XPS. This relationship further translated to improved wettability for the samples with increased surface oxygen. Notably, the deconstructed C_{1s} XPS spectrum for the untreated sample indicated two binding environments corresponding to C–C/C–H and C–O. After H_2O plasma treatment, the C–O contribution increased and C═O and

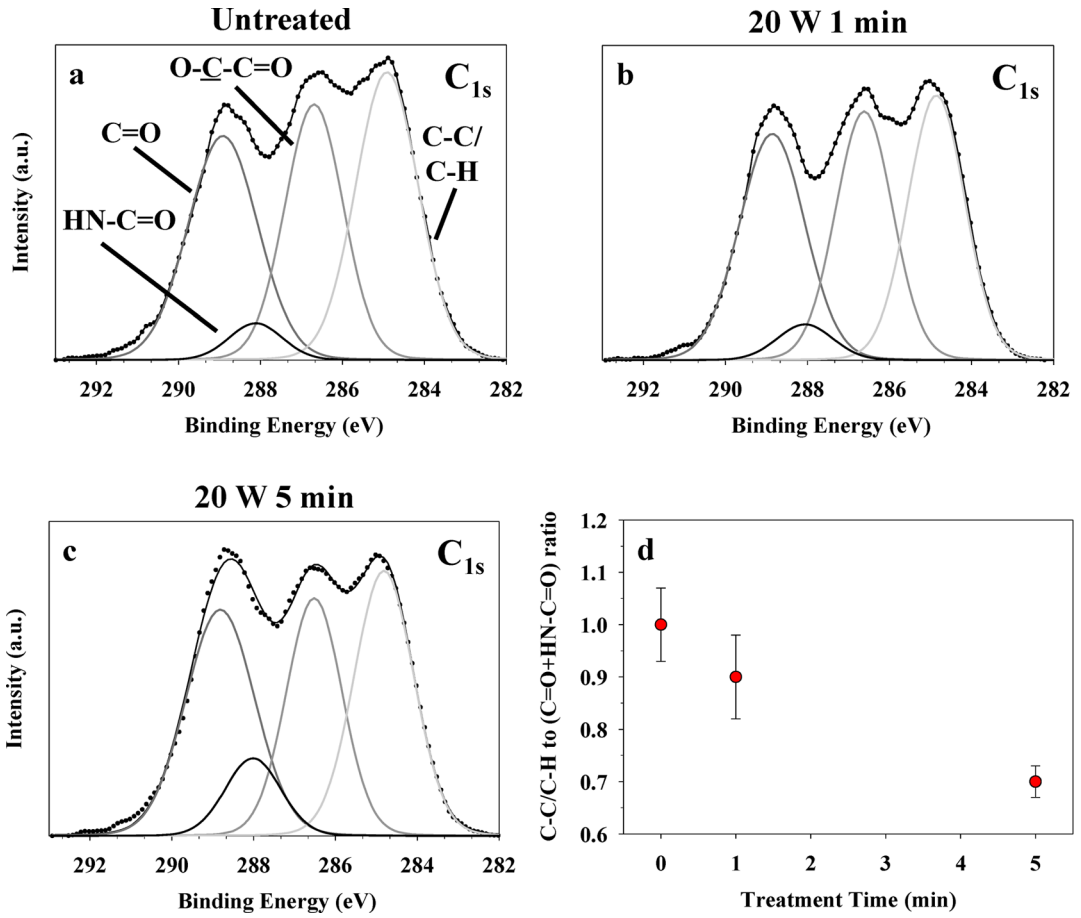

Figure 3. High-resolution C_{1s} XPS spectra and fits for (a) untreated, (b) 20 W 1 min treated, and (c) 20 W 5 min treated *S*-nitrosated PLGH-cysteine films. (d) C−C/C−H to (C═O + HN−C═O) binding environment ratios as a function of treatment time (P = 20 W). Error bars represent ±1 standard deviation (N = 6).

Table 3. Binding Environment Ratios for the Untreated and 20 W Treated Films with Different Treatment Times As Determined from the Deconstructed C_{1s} XPS Spectra[a]

treatment time (min)	C−C/C−H to C═O	C−C/C−H to O−C−C═O	C−C/C−H to HN−C═O
0	1.13 ± 0.08	1.14 ± 0.06	10.12 ± 2.03
1	1.06 ± 0.12	1.12 ± 0.12	7.10 ± 0.71
5	0.90 ± 0.06	1.15 ± 0.08	4.55 ± 0.83

[a]All analyses were performed for N = 6; the means ± standard deviation are reported.

O−C═O binding environments appeared.[50] These data suggested that polymer treatment via H_2O plasma treatments resulted in the formation of alcohol, aldehyde/ketone, and carboxylic acid/ester functionalities at the material surface, which increased the surface wettability of the samples. Translating these findings to our *S*-nitrosated PLGH-cysteine system, we can infer a direct correlation likely exists between the increase in the surface oxygen content and surface wettability. This is discussed further in section 3.4.

The notable increase in the C═O environment relative to the C−C/C−H binding environment after a 20 W, 5 min plasma treatment observed here can be understood by considering possible oxidation sites on the polymer. Previous work in our group demonstrated smaller changes in the C−O binding environment for H_2O plasma treated polysulfone materials, with a more significant impact on the C═O/O−C═O groups, such as the aldehyde/ketone and carboxylic acid/ester functional groups.[22] These data suggested the possibility of oxidation of alcohol groups formed during the treatment, or the oxidation of other sites within the polymer backbone, such as methyl groups and quaternary carbon sites, to yield aldehydes and ketones, respectively. Further oxidation of aldehydes could result in carboxylic acid groups. Other studies demonstrated surface functionalization using H_2O plasma treatments for polymers with rigid, aromatic backbones versus linear, hydrocarbon backbones.[23] In all cases, binding environments and relative elemental compositions similar to those seen here were obtained. Formation of highly oxidized species is supported by the data presented here, where we saw a notable decrease in the C−C/C−H to C═O ratio, with no distinguishable difference in the C−C/C−H to O−C−C═O ratio when comparing an untreated and 20 W, 5 min treated sample. This suggests the oxidation sites associated with the *S*-nitrosated PLGH-cysteine are likely the methyl groups of the lactic acid portion, the secondary carbon sites of the glycolic acid and HMPA portions, and the quaternary carbon site in the

HMPA portion to form ketone and aldehyde functional groups (Figure 1).

Another study demonstrated that, at lower P (e.g., 25 W), the OES spectrum as a function of plasma treatment time showed the O· signal dropped by ∼80% when the sample was introduced, which is more significant than the drop in OH·, indicating that the key player at lower applied powers is O·.[23] Additionally, there were notable differences in the resulting functionalities after plasma treatment depending on the specific material being treated. Differences in the % O incorporated and the corresponding extent of oxidation were attributed to the initial polymer structure and the number of oxidizable sites, in addition to the ability of certain polymers to undergo hydrolysis in aqueous environments. The possibility of polymer chain scission at ester sites was also acknowledged. As *S*-nitrosated PLGH-cysteine is composed of several ester linkages, it could easily undergo acid or base catalyzed hydrolysis to form carboxylic acid groups (Figure 4) and ultimately result in chain scission.[57]

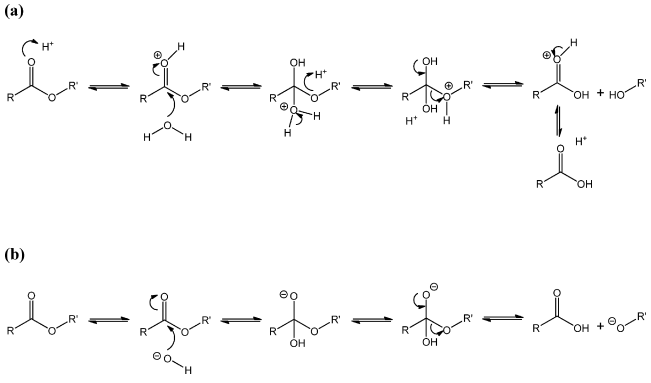

Figure 4. (a) Acid catalyzed ester hydrolysis occurs due to reaction with H^+ and H_2O species and yields carboxylic acid and alcohol products. (b) Base catalyzed ester hydrolysis occurs due to reaction with OH^- and yields carboxylic acid and alkoxide products.

Overall, the XPS data suggest combined pathways that could lead to increased hydrophilicity and thereby greater cell affinity for the *S*-nitrosated PLGH-cysteine films surfaces after plasma treatment. An increase in N content relative to both O and C content, combined with a decrease in the ratio of C−C/C−H to HN−C═O with increasing treatment time, suggests polymer rearrangement to reorient the amide linked, hydrophilic *S*-nitrosocysteine pendant groups to the surface. Additionally, an increase in the surface O, specifically the ratio of C−C/C−H to C═O, suggests implantation of OH groups at the alkyl sites along the polymer backbone, which subsequently oxidize to carbonyl sites, including ketone/aldehyde and carboxylic groups. Additionally, chain scission via ester hydrolysis is a possibility due to the large number of ester sites on the backbone.

3.2. Effect of Prolonged Treatment Time on Surface Composition. As we found greater changes occurred in film chemistry with prolonged plasma exposure, we increased treatment time to 60 min to explore parameter extremes. PLGH-cysteine films were prepared and treated for 5 or 60 min at 20 W. Because the RSNO is not contributing significantly to any of the binding environments under analysis, the thiol does not need to be nitrosated to probe functionality differences before and after treatment. Thus, non-nitrosated PLGH-cysteine films were prepared to simplify these experiments. A representative high resolution C_{1s} spectrum for a PLGH-cysteine film treated at P = 20 W for 60 min along with the C/O ratios for both the *S*-nitrosated and non-nitrosated PLGH-cysteine films as a function of treatment time are shown in Figure 5, which clearly indicates that C/O ratio decreases with increasing treatment time out to 60 min for non-nitrosated PLGH-cysteine films. There is, however, no statistical change in the C−C/C−H to HN−C═O ratio for the 5 and 60 min treated samples. This suggests no further rearrangement or functionalization occurs at prolonged treatment times, but that surface etching may be occurring.

To evaluate the hypothesis that implantation of OH and C═O groups occurs with longer plasma treatment times, polymer samples were treated and analyzed using ATR-IR. We again utilized non-nitrosated PLGH-cysteine films for these analyses to simplify the analysis. Our initial results for films treated with P = 20 W for 5 min yielded no significant changes in the IR spectrum compared to untreated films. This is most likely because of the minimal functionalization compared to the bulk (see Supporting Information, Figure S6). We thus extended treatment time to 60 min to enhance the signal of any functional groups formed during plasma treatment. Figure 6 highlights changes in the IR spectrum at 3300−3200 and 800

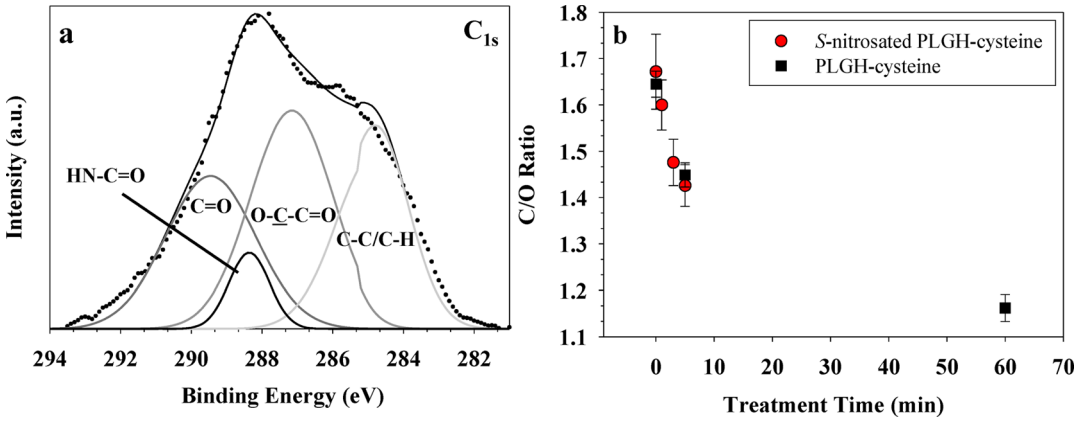

Figure 5. (a) Representative high-resolution C_{1s} XPS spectrum with deconstructed fits for a PLGH-cysteine film (60 min treatment time, P = 20 W). (b) C/O ratios as a function of treatment time (P = 20 W) for films of *S*-nitrosated and non-nitrosated PLGH-cysteine films (error bars represent ±1 standard deviation, N = 6).

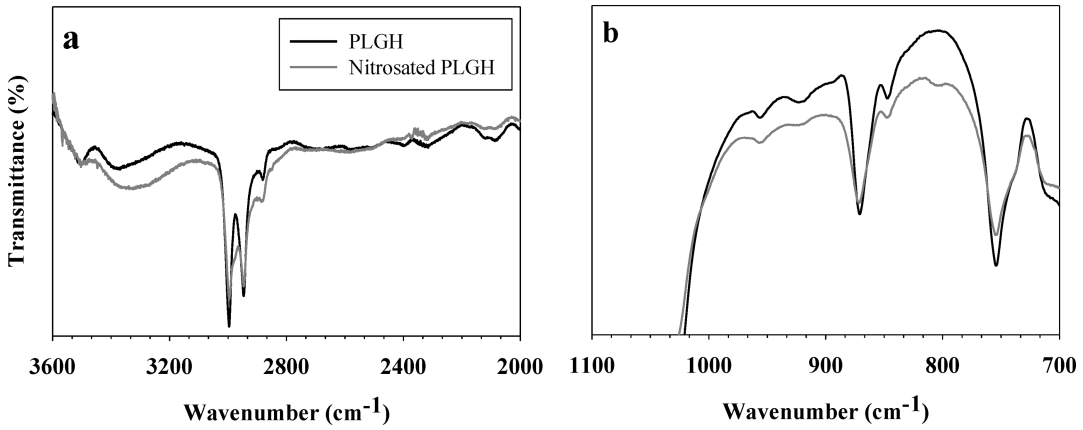

Figure 6. Representative IR spectra for untreated PLGH-cysteine (solid) and PLGH-cysteine after a 20 W, 60 min plasma treatment (dashed) for the (a) 3600−2000 cm^{-1} and (b) 1100−700 cm^{-1} regions.

cm^{-1}, corresponding to the OH stretching and out-of-plane bending modes, respectively, for alcohol and carboxylic acid groups. The PLGH-cysteine spectrum exhibits a strong absorbance at 1750 cm^{-1}, corresponding to the carbonyl groups on the polymer. As this feature is present in all spectra, we cannot deduce changes in the C═O content after plasma treatment. Nonetheless, the IR analysis suggests that H_2O plasma treatment indeed results in the incorporation of OH into the PLGH polymer structure, likely due to the formation of carboxylic acid groups, similar to what has been observed previously with other polymers.

3.3. Effect of Plasma Treatment on Surface Wettability. To assess the effect of H_2O plasma treatments on the surface wettability of the *S*-nitrosated polymer films, static WCA measurements were performed. The untreated samples exhibited a relatively high WCA of 116.6 ± 3.4°, indicating these polymers have very hydrophobic surfaces. After plasma treatment, the surfaces became hydrophilic, with the water droplet spreading completely in <100 ms (i.e., equilibrium contact angle = 0°). To distinguish between different treatments in a semiquantitative manner, we report water droplet spreading times for plasma treated surfaces in Table 4.

Table 4. Water Droplet Spreading Times Associated with Plasma Treated Samples[a]

plasma treatment		
applied rf power (W)	treatment time (min)	spreading time (ms)
20	1	87 ± 16
20	3	65 ± 13
20	5	43 ± 07
30	5	49 ± 13
50	5	70 ± 08

[a]All analyses were performed for $N = 3$, where the means ± standard deviation are reported.

Figure 7a highlights that increasing the treatment time from 1 to 5 min resulted in faster water spreading, as indicated by a lower spreading time (all with $P = 20$ W). Water droplet spreading time for the 5 min treatment was just 43 ± 7 ms, compared to 87 ± 16 ms for the 1 min treatment. Although we consider both of these surfaces to be hydrophilic, the spreading time values do suggest longer treatment time results in a more hydrophilic surface. The increase in hydrophilicity upon plasma treatment can be attributed to multiple factors. Namely, H_2O plasma treatment implants hydroxyl and carbonyl groups which can serve to increase surface hydrophilicity.[21] Additionally, plasma treatments can initiate shallow reorientation of the polymer microdomains,[56] wherein the more hydrophilic regions are brought to the surface of the film.

For a fixed treatment time of 5 min, changing P (20, 30, or 50 W) reveals a slight increase in water spreading time with increasing power (Figure 7b), although there is no significant change in water spreading time between the 20 and 30 W treatments. When P is increased to 50 W, however, the water spreading time increases significantly. This effect at the highest P could result from a competition between implantation of OH functional groups and some etching of the polymer surface, which has been previously demonstrated.[23]

3.4. Effect of Plasma Treatment on Surface Morphology. Often, plasma treatment of polymers can result in extensive changes to surface morphology, including increased surface roughness, pitting, and formation of protrusions.[23] These changes can affect both surface wettability and interactions of biological components with a material surface.[16,58−60] Thus, evaluating surface morphology and topography is critical not only from the viewpoint of biological applications, but also to ensure that observed changes in surface properties were not solely attributable to changes in surface morphology as a result of plasma treatment. Surface roughness exists perpendicular to the surface (described as height deviation), and in the plane of the surface (described by spatial parameters and identified as texture).[61] Amplitude parameters are critical to characterize surface topography for biological application, and they include the arithmetic average (R_a) and root-mean-square (R_q).[62,63] Table 5 summarizes the roughness parameters (R_a and R_q) of the *S*-nitrosated PLGH-cysteine films prior to and after treatment. No significant changes in the roughness were measured, regardless of plasma parameters used to treat the polymers. Likewise, there are no discernible differences (e.g., pitting) in the SEM images of the film surfaces, Figure 8. These observations and the insignificant changes in roughness parameters (R_a and R_q) after plasma treatment demonstrate that the observed changes in surface wettability cannot be attributed to morphological changes. This also illustrates that any etching of the surface that occurs during the 50 W treatment does not significantly affect the overall topography of the films. It is, however, well-established that surface microtopography can either promote or inhibit surface/cells interactions, depending on the specific material (i.e.,

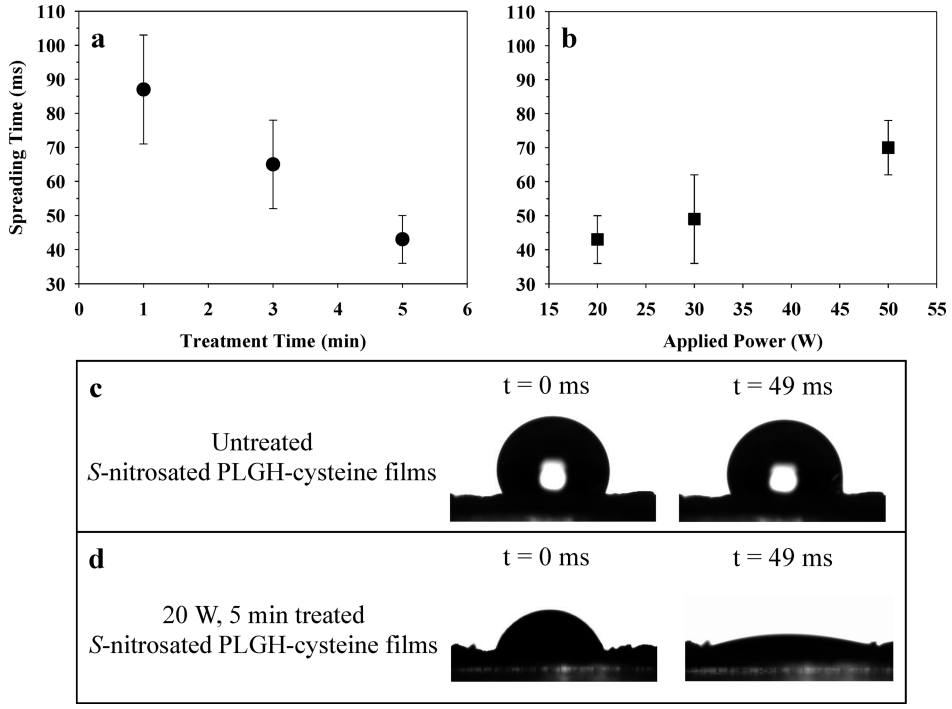

Figure 7. (a) Treatment time (P = 20 W) vs water droplet spreading time, and (b) applied power (treatment time =5 min) vs water droplet spreading time for *S*-nitrosated PLGH-cysteine films. Additionally, representative images of water droplets on (c) untreated and (d) plasma treated *S*-nitrosated PLGH-cysteine films 0 and 49 ms after a 6 μL drop has been placed on the surface. Error bars in (a) and (b) represent ±1 standard deviation (N = 3).

Table 5. Surface Roughness of Untreated and Plasma Treated *S*-Nitrosated PLGH-Cysteine Films[a]

plasma treatment			
applied rf power (W)	time (min)	R_q (μm)	R_a (μm)
		18.02 ± 6.92	14.26 ± 6.76
20	1	17.89 ± 4.56	13.73 ± 3.68
20	3	20.45 ± 3.49	16.45 ± 3.08
20	5	15.01 ± 4.84	10.96 ± 3.51
30	5	17.85 ± 3.91	13.63 ± 3.49
50	5	18.57 ± 6.12	13.82 ± 4.48

[a]All analyses were performed for N = 3, where the means ± standard deviation are reported.

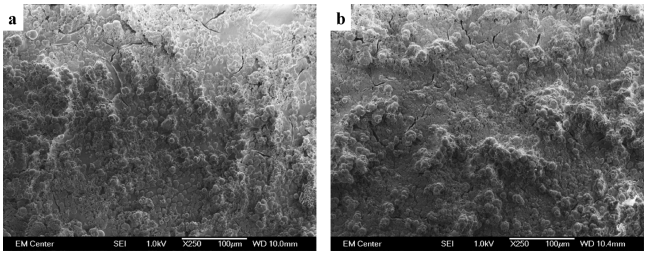

Figure 8. Representative SEM images of (a) untreated and (b) 20 W, 5 min treated *S*-nitrosated PLGH-cysteine films (both at 250× magnification).

surface chemistry) and the cell type.[64−66] Thus, surface roughness of these films is a parameter that must be considered and tuned to each intended application.

3.5. Effect of Plasma Treatment on *S*-Nitrosothiol Content and NO Release. The above sections detail extensive characterization studies that demonstrate our H_2O plasma treatments are effective at implanting functional groups in the surface of the *S*-nitrosated PLGH-cysteine films without altering bulk properties or damaging the surface of the material. These surface modifications will not be relevant, however, unless we retain the NO releasing capabilities of this model polymer system after plasma treatment. To assess these capabilities, the *S*-nitrosothiol functionality was quantified using UV−vis spectroscopy. Direct chemiluminescent detection was used to quantify the real-time NO release under dry, thermal conditions.

Figure 9 shows a representative UV−vis spectrum corresponding to the *S*-nitrosated PLGH-cysteine polymer dissolved in 2 MeOH/1 DCM, where the characteristic absorbance feature at 335 nm corresponds to the SNO moiety of the *S*-nitrosated polymer. We previously determined a molar

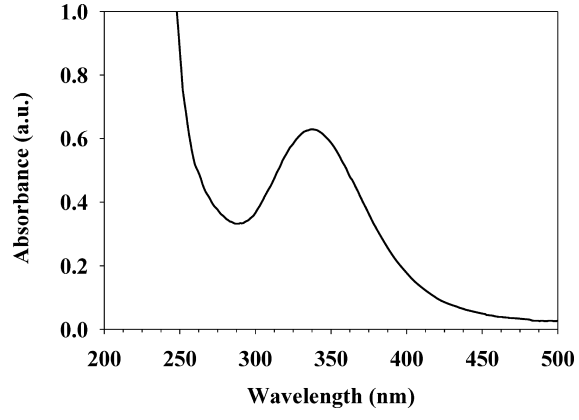

Figure 9. Representative UV−vis spectrum for untreated *S*-nitrosated PLGH-cysteine (3.5 mg mL^{-1} in 2 MeOH/1 DCM).

extinction coefficient value (ε_{max}) of 882.9 ± 18.2 M^{-1} cm^{-1} corresponding to the λ_{max} of 335 nm,[43] which allowed us to characterize an initial RSNO content of 0.155 ± 0.004 mmol g^{-1} after polymer nitrosation (Table 6). The modified Ellman's assay quantified 0.458 ± 0.009 mmol thiol g^{-1} (see Supporting Information, Figure S1), which represents a nitrosation efficiency of nearly 35%. These values correlate with previously reported values and confirm a satisfactory nitrosation of the polymer,[43] which allows us to attribute any observed variances in the RSNO content after treatment to the surface modification.

Table 6. RSNO Content and NO Recovery for Plasma Treated, *S*-Nitrosated PLGH-Cysteine Films[a]

plasma treatment			
applied power (W)	treatment time (min)	RSNO content (mmol g^{-1})[b]	NO recovery (mmol g^{-1})[c]
untreated		0.155 ± 0.004	0.012 ± 0.001
20	1	0.141 ± 0.007	0.013 ± 0.001
20	3	0.136 ± 0.005	0.011 ± 0.001
20	5	0.138 ± 0.004	0.012 ± 0.001
30	5	0.132 ± 0.005	0.011 ± 0.001
50	5	0.126 ± 0.003	0.011 ± 0.002

[a]All analyses were performed for N = 3; the means ± standard deviation are reported. [b]RSNO content determined from solution phase UV−vis measurements of the *S*-nitrosated PLGH-cysteine films dissolved in 2 MeOH/1 DCM (molar extinction coefficient of 882.9 M^{-1} cm^{-1}). [c]NO recovery is reported for dry films under 37 °C for a 12 h analysis duration.

The RSNO content was subsequently quantified for *S*-nitrosated polymer samples exposed to different H_2O plasma treatments, all of which resulted in a slight variation in the RSNO content compared to the nontreated samples; see Table 5. The Student's t test reveals, however, that for films treated at P = 20 W, regardless of treatment time (1, 3, or 5 min), the RSNO content values were the same within experimental error at the 90% CL. At P = 50 W and 5 min treatment time, a more significant decrease in the RSNO content was exhibited, with this treatment yielding an ∼80% retention of the RSNO content. Traditionally, use of *S*-nitrosothiol donors has been viewed as limited because of the minimal stability of the donor as RSNOs decompose under heat and light initiated conditions.[67] We previously demonstrated, however, that these *S*-nitrosated PLGH polymers retained their NO releasing capabilities after being processed into electrospun nanofibers.[68] The current results further demonstrate the ability of the RSNO functionality to survive processing under plasma conditions, as the RSNO content for most of the treatments was within an experimental error under the vacuum, UV light, temperature, and reactivity conditions associated with our H_2O plasma treatments.

The NO releasing parameters for any polymer system are largely controlled by the type and concentration of donor; here we have demonstrated an insignificant variance in the RSNO content (a loss of ∼10% RSNO content which corresponds to experimental error at the 90% CL) for the lower applied rf power plasma treatments. The NO release kinetics can, however, be affected by the chemical environment surrounding the RSNO group.[43] It was, therefore, critical to monitor not only the RSNO content, but the real-time NO release profile associated with the *S*-nitrosated PLGH-cysteine films. Figure 10 highlights the NO release profile for the untreated *S*-nitrosated PLGH-cysteine films under dry conditions, where a characteristic profile of an initial "burst" of NO is followed by a rather steady-state NO release. Over the 12 h analysis window, 0.012 ± 0.001 mmol NO g^{-1} was released, corresponding to ∼8% of the total NO reservoir relative to the initial RSNO content. No significant difference was found in the NO release profile or total NO release over 12 h for all of the plasma treated films compared to the untreated control (Table 6). Overall, these data demonstrate that, regardless of plasma power (P = 20−50 W) and treatment time (1−5 min), the polymers still maintained their full NO releasing capabilities in terms of the NO release kinetics under dry conditions.

To consider the NO release conditions under more physiologically relevant conditions, trials were also performed wherein films were exposed to phosphate buffered saline (PBS) over a 24 h duration. As shown in Figure 10c, the nitrosated films still exhibit the characteristic "burst" profile; however, the maximum NO release point reaches nearly 2 × 10^{-5} mmol g^{-1}, whereas the that for films exposed to only dry conditions is 3 × 10^{-6} mmol NO g^{-1}. Over the course of a 24 h buffer soak, control films (n = 5) released 0.0602 ± 0.006 mmol NO g^{-1}, whereas plasma-treated films (n = 5, 20 W, 5 min) released 0.0307 ± 0.002 mmol NO g^{-1}.

Interestingly, the NO release profiles for the films exposed to PBS are enhanced to result in a higher delivery dosage of NO compared to the dry, thermal conditions. These delivery differences can be attributed to the mechanisms associated with the NO release due to RSNO decomposition. Indeed, many RSNO decomposition triggers are known, including light, copper ion, heat, and pH.[67] More specifically, for films exposed to dry, thermal conditions, the predominant mechanism will

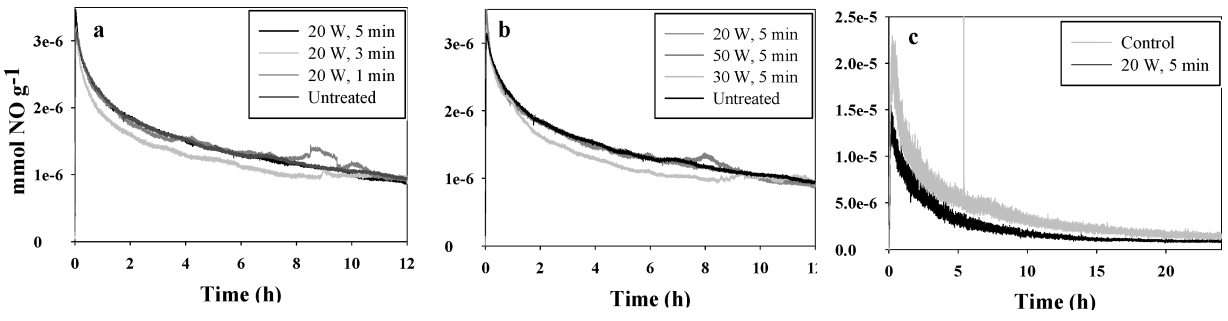

Figure 10. NO release profiles for untreated and plasma treated *S*-nitrosated PLGH cysteine polymer films treated for (a) 1, 3, or 5 min at P = 20 W; (b) 5 min at P = 20, 30, or 50 W; and (c) 5 min at P = 20 W followed by a 24 h PBS soak. Average NO release profiles are shown (N = 3), and error for all profiles is <±10%.

only involve thermal RSNO decomposition. Although no studies have considered the rate constant associated with RSNO decay under dry, thermal conditions, aqueous based studies demonstrated that, for a 10-fold concentration difference, the initial rate constant also changed by an order of magnitude.[69] As the plasma treatment results in the loss of only 10−20% of the RSNO content, it is not surprising that the NO profiles do not change significantly pre- and post-plasma treatment. Notably, the plasma treatment is surface specific and will not change the bulk of the material. As the thermal-initiated mechanism does not require surface interactions with the surroundings at a constant temperature, the profiles will be similar regardless of surface modification. In contrast, the films exposed to buffer yielded NO as a result of a pH-mediated decomposition, with trace levels of copper ion present in the buffer solution also likely contributing.

Studies considering the effect of solution pH on RSNO decomposition demonstrated a significant loss of RSNO in the pH range 7.3−7.45 compared to lower or higher values,[70] which corresponds to the pH of the buffer solution. Additionally, our Millipore treated water has been tested via ICP-OES and demonstrated 0.29 μg L^{-1} copper content.[71] The presence of copper ion will catalyze the decomposition of RSNO species; thus, trace levels of copper will result in significant decomposition of RSNO sites.[72] As both pH and copper mediated RSNO decomposition depends on uptake of the buffer solution by the film, the more hydrophilic surface created by plasma treatment will result in quicker uptake to accelerate the NO release, likely yielding the lower NO yield for the plasma-treated film compared to the control.

To determine the physiological relevance of these NO release profiles, the maximum NO point ($\sim 2 \times 10^{-5}$ mmol g^{1}) and average steady-state release after the initial burst ($\sim 2 \times 10^{-6}$ mmol g^{1}) were converted to flux values by normalizing the NO release by the surface area of the film. Using digital calipers (Fisher Scientific), an average diameter of 12.03 ± 0.04 mm (n = 6) was converted to a surface area of 1.14 ± 0.01 cm^2. The point of maximum NO release corresponds to a flux of ∼0.75 nmol min^{-1} cm^{-2}, whereas the steady state release is on the order of 0.075 nmol min^{-1} cm^{-2}. These values fall within the range of the NO flux of the natural endothelium, which releases 0.05−0.4 nmol NO cm^{-2} min^{-1},[73,74] and serves as the therapeutic target threshold for NO releasing materials. Therefore, these materials, when exposed to buffer and regardless of plasma treatment, still release an NO flux that is physiologically valid.

3.6. Stability of the Plasma Treatment. Plasma treated surfaces can undergo what is generally referred to as hydrophobic recovery, wherein surfaces that are rendered hydrophilic ultimately revert to their original hydrophobic nature shortly after the treatment.[54−56] This is generally thought to occur via polymer rearrangement, chain migration or diffusion, or burial of hydrophilic groups (e.g., O, N) within the bulk of the polymer. To examine aging effects with our materials, *S*-nitrosated PLGH-cysteine films were plasma treated (P = 20 W, 5 min) and then placed into a freezer at −18 °C under ambient conditions for a 10 day aging period. These conditions were chosen to minimize the decomposition of the RSNO during storage, while still being able to assess the treatment stability. Hydrophobic recovery of stored samples was assessed by WCA and XPS measurements, and the results were compared to untreated and freshly treated samples. Water spreading time on the plasma treated material after the 10-day storage period was 249 ± 33 ms, significantly longer than that on freshly treated films (43 ± 7 ms). Despite this increase in the water spreading time, these surfaces are considered very hydrophilic as the water droplet still spreads extremely rapidly on the surface.

XPS analysis reveals the 10-day storage resulted in a significant increase in the O/N (17.8 ± 1.4), C/N (27.5 ± 2.3), and C/O (1.54 ± 0.02) ratios compared with those of freshly treated samples, Table 2. These differences in the elemental ratios between freshly treated and aged samples were normalized by the elemental ratio for the untreated samples to yield 32, 34, and 7% changes for the O/N, C/N and C/O ratios, respectively. This suggests slight hydrophobic recovery may be the result of burial of the N-containing hydrophilic cysteine microdomains accompanied by some burial of surface O-containing moieties. Furthermore, the C/O ratio is larger for the untreated sample than the 10 day aged sample, which suggests that oxygen-containing functional groups implanted via plasma treatment are maintained even after the 10 day storage period.

In addition to the stability and longevity of the plasma-induced compositional changes, the stability of the RSNO group will also dictate the lifetime of these materials for bioapplications. After the storage period, the RSNO content was 0.126 ± 0.003 mmol g^{-1} compared to 0.138 ± 0.004 mmol g^{-1} for freshly treated films. The 20 W, 5 min treatment resulted in ∼10% decrease in the RSNO content compared to untreated films and the storage period resulted in the loss of an additional 10%, leaving ∼80% of the original RSNO content remaining after plasma treatment and storage. Despite an additional decrease in RSNO content, the real-time NO release profile and total NO release over a 12 h period was comparable to all other freshly treated films.

We have previously demonstrated that H_2O plasma treated polymeric materials can exhibit either minor changes in hydrophilicity over extended periods of time or complete hydrophobic recovery over time due to polymer rearrangement, depending on the material. For example, H_2O plasma treatments have resulted in permanent hydrophilic modifications (lasting months to years) for polymers with more rigid, aromatic backbones, such as polysulfone, polycarbonate, and polyethylene terephthalate.[22−24] The less rigid polyethylene materials, however, experienced significant hydrophobic recovery after only 48 h to 1 week as the migration of polymer chains effectively buried the polar surface groups incorporated during H_2O plasma treatment. Comparatively, although plasma treated *S*-nitrosated polymer films exhibit a small amount of hydrophobic recovery, they still maintain their overall hydrophilic nature. These aging studies clearly indicate that our materials are relatively stable in terms of wettability and surface functionality. This result is significant in that other nonaromatic backbone polymers exposed to H_2O plasma treatment exhibited nearly complete immediate hydrophobic recovery in terms of the WCA.[23] Here, we present the H_2O plasma treatment of a nonrigid polymer that still retains a hydrophilic surface. Future studies will translate this work to NO-releasing polymer systems with even more rigid backbones with the goal of designing even more stable materials for biological applications.

4. CONCLUSIONS

Overall, we report the ability to tailor the surface properties of a model NO-releasing polymer while still maintaining the NO

release capability. H_2O plasma treatments effectively modified the surface wettability of *S*-nitrosated PLGH-cysteine films, creating much more hydrophilic surfaces. We demonstrated that, for $P \leq 30$ W, the NO reservoir in the form of *S*-nitrosothiol was within error of the untreated films, and the NO release kinetics were not altered via plasma modification. Only at the highest applied rf powers, $P = 50$ W, was an additional loss of RSNO observed. When comparing the NO release initiated by a buffer soak, the plasma-treated films did exhibit a decrease in NO recovery compared to the control; however, the plasma-treated materials still released NO in the range associated with the natural endothelium. XPS analysis revealed an increase in N signal relative to O and C, which indicates the rearrangement of the polymer exposing hydrophilic cysteine residues on the film surface. The observed decreasing trend in the C/O ratio likely results from conversion of pre-existing carbonyl groups to hydroxyl groups. Additional IR analysis of films plasma treated for 60 min demonstrated the appearance of features corresponding to the incorporation of OH functional groups. Surface roughness analysis indicated no significant changes in the surface morphology after plasma treatment, supporting that the changes in surface wettability are primarily due to changes in chemical functionality. Notably, plasma treated surfaces remain hydrophilic after a 10 day storage period in the freezer (−18 °C), which suggests that the films do not experience short-term hydrophobic recovery. Overall, the ability to tune the surface wettability of a polymer film while maintaining the bulk properties, including NO therapeutic releasing parameters and the stability of the treatment over time, is critical toward creating multifunctional biomaterial systems. Future studies include evaluating the cell−surface interactions of these materials as well as investigating long-term antimicrobial activity and plasma treatment of other polymers with NO-releasing capabilities.

■ ASSOCIATED CONTENT

Supporting Information

Ellman's assay for thiol quantification; *S*-nitrosothiol characterization, baseline PLGH-cysteine calibration curve; SEM-EDS analysis; XPS analysis; IR analysis. This material is available free of charge via the Internet at http://pubs.acs.org.

■ AUTHOR INFORMATION

Corresponding Author

*E-mail: Ellen.Fisher@ColoState.Edu.

Notes

The authors declare no competing financial interest.

■ ACKNOWLEDGMENTS

The authors gratefully acknowledge funding received from Colorado State University, the Department of Defense Congressionally Directed Medical Research Program (DOD-CDMRP), and the National Science Foundation (DMR-0847641 and CHE-1152963). We thank Dr. Patrick McCurdy of the CSU Chemistry Central Instrument Facility for XPS, SEM, and EDS support and Mr. John Wydalis and Prof. Charles Henry's research group at CSU for profilometry technical support. Mr. Alec Lutzke assisted with NMR data collection and interpretation (not shown). This research was further supported by funds from the Boettcher Foundation's Webb-Waring Biomedical Research Program. J.M.J. was supported by the Boettcher Foundation's Webb-Waring Biomedical Research Program. A.P.-J. and M.J.H. were supported by NSF CHE-1152963.

■ REFERENCES

(1) Ratner, B. D. The Blood Compatibility Catastrophe. *J. Biomed. Mater. Res.* **1993**, *27*, 283−287.
(2) Ratner, B. D. The Catastrophe Revisited: Blood Compatibility in the 21st Century. *Biomaterials* **2007**, *28*, 5144−5147.
(3) Anderson, J. M. Biological Responses to Materials. *Annu. Rev. Mater. Res.* **2001**, *31*, 81−110.
(4) Costerton, J. W.; Steward, P. S.; Greenberg, E. P. Bacterial Biofilms: A Common Cause of Persistent Infections. *Science* **1999**, *284*, 1318−1322.
(5) Donlan, R. M. Biofilms and Device-associated Infections. *Emerging Infect. Dis.* **2001**, *7*, 277−281.
(6) Frost, M. C.; Reynolds, M. M.; Meyerhoff, M. E. Polymers Incorporating Nitric Oxide Releasing/Generating Substances for Improved Biocompatibility of Blood-contacting Medical Devices. *Biomaterials* **2005**, *26*, 1685−1693.
(7) Pashkuleva, I.; Marques, A. P.; Vaz, F.; Reis, R. L. Surface Modification of Starch Based Biomaterials by Oxygen Plasma or UV-irradiation. *J. Mater. Sci.: Mater. Med.* **2010**, *21*, 21−32.
(8) Arima, Y.; Iwata, H. Effect of Wettability and Surface Functional Groups on Protein Adsorption and Cell Adhesion Using Well-defined Mixed Self-assembled Monolayers. *Biomaterials* **2007**, *28*, 3074−3082.
(9) Castner, D. G.; Ratner, B. D. Biomedical surface science: Foundations to frontiers. *Surf. Sci.* **2002**, *500*, 28−60.
(10) Van Loosdrecht, M. C.; Lyklema, J.; Norde, W.; Schraa, G.; Zehnder, A. The Role of Bacterial Cell Wall Hydrophobicity in Adhesion. *Appl. Environ. Microbiol.* **1987**, *53*, 1893−1897.
(11) Bruinsma, G. M.; van der Mei, H. C.; Busscher, H. J. Bacterial Adhesion to Surface Hydrophilic and Hydrophobic Contact Lenses. *Biomaterials* **2001**, *22*, 3217−3224.
(12) Okada, T.; Bark, D. H.; Mayberg, M. R. Local Anticoagulation without Systems Effect using a Polymer Heparin Delivery System. *Stroke* **1988**, *19*, 1470−1476.
(13) Uhrich, K. E.; Cannizzaro, S. M.; Langer, R. S.; Shakesheff, K. M. Polymeric Systems for Controlled Drug Release. *Chem. Rev.* **1999**, *99*, 3181−3198.
(14) Hetrick, E. M.; Schoenfisch, M. H. Reducing Implant-Related Infections: Active Release Strategies. *Chem. Soc. Rev.* **2006**, *35*, 780−789.
(15) Luscher, T. F.; Steffel, J.; Eberli, F. R.; Joner, M.; Nakazawa, G.; Tanner, F. C.; Virmani, R. Drug-eluting Stent and Coronary Thrombosis: Biological Mechanisms and Clinical Implications. *Circulation* **2007**, *115*, 1051−1058.
(16) Parreira, P.; Magalhães, A.; Gonçalves, I. C.; Gomes, J.; Vidal, R.; Reis, C. A.; Leckband, D. E.; Martins, M. C. L. Effect of Surface Chemistry on Bacterial Adhesion, Viability, and Morphology. *J. Biomed. Mater. Res., Part A* **2011**, *99*, 344−353.
(17) Kenawy, E. R.; Worley, S. D.; Broughton, R. The Chemistry and Applications of Antimicrobial Polymers: A State-of-the-Art Review. *Biomacromolecules* **2007**, *8*, 1359−1384.
(18) Beck, A. J.; Whittle, J. D.; Bullett, N. A.; Eves, P.; MacNeil, S.; McArthur, S. L.; Shard, A. G. Plasma Co-polymerisation of Two Strongly Interacting Monomers: Acrylic Acid and Allylamine. *Plasma Processes Polym.* **2005**, *2*, 641−649.
(19) Sohbatzadeh, F.; Hosseinzadeh Colagar, A.; Mirzanejhad, S.; Mahmodi, S. *E. coli*, *P. aeruginosa*, and *B. cereus* Bacteria Sterilization using Afterglow of Non-thermal Plasma at Atmospheric Pressure. *Appl. Biochem. Biotechnol.* **2010**, *160*, 1978−1984.
(20) Griesser, H. J.; Hodgkin, J. H.; Schmidt, R. *Progress in Biomedical Applications*; Plenum Press: New York, 1990; p 205−215.
(21) Lee, J. H.; Park, J. W.; Lee, H. B. Cell-Adhesion and Growth on Polymer Surfaces with Hydroxyl Groups Prepared by Water-Vappor Plasma Treatment. *Biomaterials* **1991**, *12*, 443−448.
(22) Steen, M. L.; Hymas, L.; Havey, E. D.; Capps, N. E.; Castner, D. G.; Fisher, E. R. Low Temperature Plasma Treatment of Asymmetric

Polysulfone Membranes for Permanent Hydrophilic Surface Modification. *J. Membr. Sci.* **2001**, *188*, 97−114.
(23) Steen, M. L.; Jordan, A. C.; Fisher, E. R. Hydrophilic Modification of Polymeric Membranes by Low Temperature H_2O Plasma Treatment. *J. Membr. Sci.* **2002**, *204*, 341−357.
(24) Tompkins, B. D.; Dennison, J. M.; Fisher, E. R. H_2O Plasma Modification of Track-etched Polymer Membranes for Increased Wettability and Improved Performance. *J. Membr. Sci.* **2013**, *428*, 576−588.
(25) Carpenter, A. W.; Schoenfisch, M. H. Nitric Oxide Release: Part II. Therapeutic Applications. *Chem. Soc. Rev.* **2012**, *41*, 3742−3752.
(26) Radomski, M. W.; Moncada, S. The Biological and Pharmacological Role of Nitric Oxide in Platelet Function. *Adv. Exp. Med. Biol.* **1993**, *344*, 251−265.
(27) Reynolds, M. M.; Annich, G. M. The Artificial Endothelium. *Organogenesis* **2011**, *7*, 42−49.
(28) Fang, F. C. Mechanisms of Nitric Oxide-related Antimicrobial Activity. *J. Clin. Invest.* **1997**, *99*, 2818−2825.
(29) Schaffer, M. R.; Tantry, U.; Gross, S. S.; Wasserkrug, H. L.; Barbul, A. Nitric Oxide Regulates Wound Healing. *J. Surg. Res.* **1996**, *63*, 237−240.
(30) Ziche, M.; Morbidelli, L. Nitric Oxide and Angiogenesis. *J. Neuro-Oncol.* **2000**, *50*, 139−148.
(31) Rizk, M.; Witte, M. B.; Barbul, A. Nitric Oxide and Wound Healing. *World J. Surg.* **2004**, *28*, 301−306.
(32) Varu, V. N.; Tsihlis, N. D.; Kibbe, M. R. Nitric Oxide-releasing Prosthetic Materials. *Vasc. Endovasc. Surg.* **2009**, *43*, 121−131.
(33) Seabra, A. B.; Duran, N. Nitric Oxide-releasing Vehicles for Biomedical Applications. *J. Mater. Chem.* **2010**, *20*, 1624−1637.
(34) Jen, M. C.; Serrano, M. C.; van Lith, R.; Ameer, G. A. Polymer-Based Nitric Oxide Therapies: Recent Insights for Biomedical Applications. *Adv. Funct. Mater.* **2012**, *22*, 239−260.
(35) Riccio, D. A.; Schoenfisch, M. H. Nitric Oxide Release: Part I. Macromolecular Scaffolds. *Chem. Soc. Rev.* **2012**, *41*, 3731−3741.
(36) VanWagner, M.; Rhadigan, J.; Lancina, M.; Lebovsky, A.; Romanowicz, G.; Holmes, H.; Brunette, M. A.; Snyder, K. L.; Bostwick, M.; Lee, B. P.; Frost, M. C. *S*-Nitroso-*N*-acetylpenicillamine (SNAP) Derivatizaton of Peptide Primary Amines to Create Inducible Nitric Oxide Donor Biomaterials. *ACS Appl. Mater. Interfaces* **2013**, *5*, 8430−8439.
(37) Reynolds, M. M.; Frost, M. C.; Meyerhoff, M. E. Nitric Oxide-Releasing Hydrophobic Polymers: Preparation, Characterization, and Potential Biomedical Applications. *Free Radical Biol. Med.* **2004**, *37*, 926−936.
(38) Joslin, J. M.; Lantvit, S. M.; Reynolds, M. M. Nitric Oxide Releasing Tygon Materials: Studies in Donor Leaching and Localized Nitric Oxide Release at a Polymer-Buffer Interface. *ACS Appl. Mater. Interfaces* **2013**, *5*, 9285−9294.
(39) Kingshott, P.; Andersson, G.; McArthur, S. L.; Griesser, H. J. Surface Modification and Chemical Surface Analysis of Biomaterials. *Curr. Opin. Chem. Biol.* **2011**, *15*, 667−676.
(40) Yasuda, H.; Gazicki, M. Biomedical Applications of Plasma Polymerizationand Plasma Treatment of Polymer Surfaaces. *Biomaterials* **1982**, *3*, 68−77.
(41) Osaki, S. G.; Chen, M.; Zamora, P. O. Controlled Drug Release thorough a Plasma Polymerized Tetramethylcyclo-tetrasiloxane Coating Barrier. *J. Biomater. Sci., Polym. Ed.* **2012**, *23*, 483−496.
(42) Yoo, H. S.; Kim, T. G.; Partk, T. G. Surface-functionalized Electrospun Nanofibers for Tissue Engineering and Drug Delivery. *Adv. Drug Delivery Rev.* **2009**, *61*, 1033−1042.
(43) Damodaran, V. B.; Joslin, J. M.; Wold, K. A.; Lantvit, S. M.; Reynolds, M. M. S-Nitrosated Biodegradable Polymers for Biomedical Applications: Synthesis, Characterization and Impact of Thiol Structure on the Physicochemical Properties. *J. Mater. Chem.* **2012**, *22*, 5990−6001.
(44) Fortunati, E.; Mattioli, S.; Visai, L.; Imbriani, M.; Fierro, J. G.; Kenny, J. M.; Armentano, I. Combined Effects of Ag Nanoparticles and Oxygen Plasma Treatment on PLGA Morphological, Chemical, and Antibacterial Properties. *Biomacromolecules* **2013**, *14*, 626−636.
(45) Djordjevic, I.; Britcher, L. G.; Kumar, S. Morphological and Surface Compositional Changes in Poly(lactide-*co*-glycolide) Tissue Engineering Scaffolds Upon Radio Frequency Glow Discharge Plasma Treatment. *Appl. Surf. Sci.* **2008**, *254*, 1929−1935.
(46) Khorasani, M. T.; Mirzadeh, H.; Irani, S. Plasma Surface Modification of Poly(lactic acid) and Poly(lactic-*co*-glycolic acid) Films for Improvement of Nerve Cells Adhesion. *Radiat. Phys. Chem.* **2008**, *77*, 280−287.
(47) Damodaran, V. B.; Reynolds, M. M. Synthesis and Evaluation of Novel Biodegradable Multi-block Polymers for Controlled Nitric Oxide Delivery. In *Abstracts of Papers of the American Chemical Society*, American Chemical Society National Meeting, Anaheim, CA, March 27−31, 2011; American Chemical Society: Washington, DC, 2011; Vol. *241*.
(48) Damodaran, V. B.; Reynolds, M. M. Biodegradable S-nitrosothiol Tethered Multiblock Polymer for Nitric Oxide Delivery. *J. Mater. Chem.* **2011**, *21*, 5870−5872.
(49) Bates, J. N. Nitric Oxide Measurement by Chemiluminescence Detection. *Neuroprotocols* **1992**, *1*, 141−149.
(50) Asfardjani, K.; Segui, Y.; Aurelle, Y.; Abidine, N. Effect of Plasma Treatments on Wettability of Polysulfone and Polyetherimide. *J. Appl. Polym. Sci.* **1991**, *43*, 271−281.
(51) Goldstein, J.; Newbury, D.; Joy, D.; Lyman, C.; Echlin, P.; Lifshin, E.; Sawyer, L.; Michael, J. *Scanning Electron Microscopy and X-Ray Microanalysis*, 3rd ed.; Kluwer Academic Press: New York, 2007.
(52) McArthur, S. L. Applications of XPS in Bioengineering. *Surf. Interface Anal.* **2006**, *38*, 1380−1385.
(53) Ershov, S.; Khelifa, F.; Dubois, P.; Snyders, R. Derivatization of Free Radicals in an Isopropanol Plasma Polymer Film: The First Step toward Polymer Graftingq. *ACS Appl. Mater. Interfaces* **2013**, *5*, 4216−4223.
(54) Gengenbach, T.; Chatelier, R. C.; Griesser, H. J. Characterization of the Ageing of Plasma-Deposited Polymer Films: Global Analysis of X-ray Photoelectron Spectroscopy Data. *Surf. Interface Anal.* **1996**, *24*, 271−281.
(55) Tarasova, A.; Hamilton-Brown, P.; Gengengach, T.; Griesser, H. J.; Meagher, L. Colloid Probe AFM and XPS Study of Time-Dependent Aging of Amine Plasma Polymer Coatings in Aqueous Media. *Plasma Process. Polym.* **2008**, *5*, 175−185.
(56) Griesser, H. J.; Da, Y.; Hughes, A. E.; Gengenbach, T. R.; Mau, A. W. H. Shallow Reorientation in the Surface Dynamics of Plasma-treated Fluorinated Ethylene-propylene Polymer. *Langmuir* **1991**, *7*, 2484−2491.
(57) Croll, T. I.; O'Connor, A. J.; Stevens, G. W.; Cooper-White, J. J. Controllable Surface Modification of Poly(lactic-*co*-glycolic acid) (PLGA) by Hydrolysis or Aminolysis I: Physical, Chemical, and Theoretical Aspects. *Biomacromolecules* **2004**, *5*, 463−473.
(58) Thissen, H.; Johnson, G.; McFarland, G.; Verbiest, B. C. H.; Gengenbach, T.; Voelckera, N. H. Microarrays for the Evaluation of Cell-biomaterial Surface Interactions. In *Smart Materials IV*; Voelcker, N. H., Ed.; Spie-Intternational Society for Optical Engineering: Bellingham, WA, 2007; Vol. *6413*, pp B4130−B4130.
(59) Deligianni, D. D.; Katsala, N. D.; Koutsoukos, P. G.; Missirlis, Y. F. Effect of Surface Roughness of Hydroxyapatite on Human Bone Marrow Cell Adhesion, Proliferation, Differentiation and Detachment Strength. *Biomaterials* **2000**, *22*, 87−96.
(60) Quere, D. Wetting and Roughness. *Annu. Rev. Mater. Res.* **2008**, *38*, 71−99.
(61) Thomas, T. *Rough Surfaces*; World Scientific Publishing Company: London, 1999.
(62) Carneiro, K.; Jensen, C. P.; Jørgensen, J. F.; Garnoes, J.; McKeown, P. A. Roughness Parameters of Surfaces by Atomic Force Microscopy. *CIRP Ann. Manuf. Technol.* **1995**, *44*, 517−522.
(63) Peltonen, J.; Jarn, M.; Areva, S.; Linden, M.; Rosenholm, J. B. Topographical Parameters for Specifying a Three-dimensional Surface. *Langmuir* **2004**, *20*, 9428−9431.
(64) Wang, Y. X.; Robertson, J. L.; Spillman, W. B.; Claus, R. O. Effects of the Chemical Structure and the Surface Properties of

Polymeric Biomaterials on their Biocompatibility. *Pharm. Res.* **2004**, *21*, 1362−1373.
(65) Ranucci, C. S.; Prabhas, V. M. Substrate Microtopography Can Enhance Cell Adhesive and Migratory Responsiveness to Matrix Ligand Density. *J. Biomed. Mater. Res.* **2001**, *54*, 149−161.
(66) Deligianni, D. D.; Katsala, N. D.; Koutsoukos, P. G.; Missirlis, Y. F. Effect of Surface Roughness of Hydroxyapatite on Human Bone Marrow Cell Adhesion, Proliferation, Differentiation and Detachment Strength. *Biomaterials* **2000**, *22*, 87−96.
(67) Williams, D. L. H. The Chemistry of S-Nitrosothiols. *Acc. Chem. Res.* **1999**, *32*, 869−876.
(68) Wold, K. A.; Damodaran, V. B.; Suazo, L. A.; Bowen, R. A.; Reynolds, M. M. Fabrication of Biodegradable Polymeric Nanofibers with Covalently Attached NO Donors. *ACS Appl. Mater. Interfaces* **2012**, *4*, 3022−3030.
(69) de Oliveira, M. G.; Shishido, S. M.; Seabra, A. B.; Morgon, N. H. Thermal Stability of Primary S-nitrosothiols: Roles of Autocatalysis and Structural Effects on the Rate of Nitric Oxide Release. *J. Phys. Chem. A* **2002**, *106*, 8963−8970.
(70) Gu, J.; Lewis, R. S. Effect of pH and Metal Ions on the Decomposition Rate of S-Nitrosocysteine. *Ann. Biomed. Eng.* **2007**, *35*, 1554−1560.
(71) L, H. J.; Reynolds, M. M. Metal Organic Frameworks as Nitric Oxide Catalysts. *J. Am. Chem. Soc.* **2012**, *134*, 3330−3333.
(72) Askew, S. C.; Barnett, D. J.; Mcaninly, J.; Williams, D. L. H. Catalysis by Cu^{2+} of Nitric-Oxide Release from S-Nitrosothiols (RSNO). *J. Chem. Soc., Perkin Trans. 2* **1995**, 741−745.
(73) Radomski, M. W.; Palmer, R. M. J.; Moncada, S. The Role of Nitric-oxide and CGMP in Platelet-Adhesion to Vascular Endothelium. *Biochem. Biophy. Res. Commun.* **1987**, *148*, 1482−1489.
(74) Vaughn, M. W.; Kuo, L.; Liao, J. C. Estimation of Nitric Oxide Production and Reaction Rates in Tissue by Use of a Mathematical Model. *Am. J. Physiol.: Heart Circ. Physiol.* **1998**, *274*, H2163−H2176.